JB Journals.ASM.org

Structure of Microcin B-Like Compounds Produced by *Pseudomonas syringae* and Species Specificity of Their Antibacterial Action

Mikhail Metelev,[a] Marina Serebryakova,[a,b] Dmitry Ghilarov,[a] Youfu Zhao,[c] Konstantin Severinov[a,d,e]

Institute of Gene Biology of the Russian Academy of Sciences, Moscow, Russia[a]; Moscow State University, Moscow, Russia[b]; Department of Crop Sciences, University of Illinois at Urbana-Champaign, Urbana, Illinois, USA[c]; St. Petersburg State Polytechnical University, St. Petersburg, Russia[d]; Waksman Institute for Microbiology and Department of Molecular Biology and Biochemistry, Rutgers, The State University of New Jersey, Piscataway, New Jersey, USA[e]

***Escherichia coli* microcin B (*Ec*-McB) is a posttranslationally modified antibacterial peptide containing multiple oxazole and thiazole heterocycles and targeting the DNA gyrase. We have found operons homologous to the *Ec*-McB biosynthesis-immunity operon *mcb* in recently sequenced genomes of several pathovars of the plant pathogen *Pseudomonas syringae*, and we produced two variants of *P. syringae* microcin B (*Ps*-McB) in *E. coli* by heterologous expression. Like *Ec*-McB, both versions of *Ps*-McB target the DNA gyrase, but unlike *Ec*-McB, they are active against various species of the *Pseudomonas* genus, including human pathogen *P. aeruginosa*. Through analysis of *Ec*-McB/*Ps*-McB chimeras, we demonstrate that three centrally located unmodified amino acids of *Ps*-McB are sufficient to determine activity against *Pseudomonas*, likely by allowing specific recognition by a transport system that remains to be identified. The results open the way for construction of McB-based antibacterial molecules with extended spectra of biological activity.**

Microcins were originally defined as low-molecular-weight (<10-kDa) ribosomally synthesized antibacterial peptides produced by some naturally occurring strains of *Escherichia coli* (1). Microcinogenic *E. coli* strains harbor plasmids carrying clustered genes responsible for microcin synthesis and self-immunity of the producing cell. Some microcins contain highly unusual structures introduced into the ribosomally synthesized peptide precursor (promicrocin) by special enzymes (2, 3).

Bioinformatics analysis revealed that clusters of genes orthologous to microcin biosynthesis/self-immunity genes are widespread in bacteria (4, 5), while functional studies confirmed that ribosomally synthesized antibacterial peptides, including peptides with extensive posttranslational modifications, are commonly produced by diverse bacteria (6). *Escherichia coli* microcin B (*Ec*-McB), a DNA gyrase inhibitor, is a founding member of a diverse class of natural products referred to as TOMMs (thiazole-oxazole-modified microcins) (7). The thiazole and oxazole heterocycles of TOMMs are derived from cysteine and serine residues of precursor peptides.

E. coli cells producing microcin B contain plasmids carrying a 7-gene *mcb* operon. The *mcbA* gene encodes a precursor peptide; the *mcbBCD* genes encode subunits of the microcin B synthase, an enzyme responsible for the synthesis of oxazole and thiazole heterocycles (8, 9); the *mcbEF* genes encode an export pump; and *mcbG* encodes a pentapeptide repeat protein that binds to a microcin B target, the DNA gyrase, rendering it resistant to microcin B inhibition (10). The microcin B precursor, the 69-amino-acid-long McbA, contains an N-terminal leader (amino acids 1 to 26) that is recognized by the McbBCD complex. After binding to the leader, the McbBCD synthase moves in the C-terminal direction, converting the GlySer and GlyCys McbA dipeptides into oxazole and thiazole heterocycles, respectively (9). Two McbA tripeptides, GlySerCys and GlyCysSer, are converted into oxazole-thiazole and thiazole-oxazole bis-heterocycles (site A and site B), thought to be important for microcin B activity (11). *E. coli* McbA contains an additional centrally located GlyCysSer tripeptide that can be converted to a fused heterocycle (site C) but is present mostly in the form of a single thiazole heterocycle with a C-terminally located backbone ester bond connecting residues 51 and 52 (12). After completion of backbone modifications, the leader peptide is cleaved off (13), and mature 3,093-Da microcin B containing eight heterocycles is exported from the producing cell.

While microcin B targets the DNA gyrase, the targets of most TOMMs are unknown. Some of these compounds, like streptolysin S, function as bacteriolysins (14) and may therefore target cell membranes. In this work, we characterize a TOMM encoded by an *mcb*-like operon from *Pseudomonas syringae* pv. *glycinea* B076, a plant pathogen responsible for bacterial blight of soybean (15). We demonstrate that the *P. syringae* microcin B (*Ps*-McB)-like compound also targets the DNA gyrase but, unlike the *E. coli* counterpart, inhibits the growth of not just *E. coli* but also *P. syringae* and *Pseudomonas aeruginosa*. By analyzing chimeric microcins, we map the main determinant of extended bioactivity of *P. syringae* microcin B to a centrally located unmodified tripeptide, which is apparently specifically recognized by cell uptake machinery present in *Pseudomonas*. We propose that site-specific genetic modification of microcin B-like compounds may open the way for construction of DNA gyrase poisons with extended spectra of biological activity.

MATERIALS AND METHODS

Bacterial strains and growth conditions. The *E. coli* strains used in this work were DH5α [F^- *endA1 glnV44 thi-1 recA1 relA1 gyrA96 deoR nupG* ϕ80d*lacZ*ΔM15 Δ(*lacZYA-argF*)*U169 hsdR17*(r_K^- m_K^+) λ^-],

Received 4 June 2013 Accepted 4 July 2013
Published ahead of print 12 July 2013
Address correspondence to Konstantin Severinov, severik@waksman.rutgers.edu.
Supplemental material for this article may be found at http://dx.doi.org/10.1128/JB.00665-13.

doi:10.1128/JB.00665-13

BL21(DE3) {F$^-$ *ompT gal dcm lon hsdSB*(r_B^- m_B^-) λ(DE3 [*lacI lacUV5-T7* gene 1 *ind1 sam7 nin5*])}, CSH50 λ*sfiA*::*lacZ* (a CSH50 [16] λ lysogen carrying a transcriptional *sfiA*::*lacZ* fusion [13]), XL1-Blue (Stratagene) {*endA1 gyrA96*(Nal^r) *thi-1 recA1 relA1 lac glnV44* F′[::Tn*10 proAB*$^+$ *lacI*^{q} Δ(*lacZ*)M15] *hsdR17*(r_K^- m_K^+)}, and MG1655 (F$^-$ λ$^-$ *ilvG rfb-50 rph-1*). An MG1655 derivative harboring the *gyrB* gene encoding a W-to-R change at position 751 (*gyrB* W751R) (ML751) was provided by Anthony Maxwell (John Innes Centre). Derivatives of the XL1-Blue strain lacking *ompF* and *sbmA* were constructed by using the λ red system according to the method of Datsenko and Wanner (17). The source of *P. aeruginosa* strain PAO1 was described previously (18). *P. syringae* pv. *glycinea* strain B076, *P. syringae* pv. *tomato* strain DC3000, *P. syringae* pv. *syringae* strain B728a, and *P. syringae* pv. *phaseolicola* strain 1448a were obtained from the Zhao laboratory collection (19–21).

Bacteria were grown in LB rich medium or in M9 minimal medium supplemented with the appropriate carbon source. MacConkey lactose plates (1.35% agar) were prepared according to the manufacturer's instructions (BBL).

Molecular cloning procedures. A 5.3-kb DNA fragment containing the entire *P. syringae mcb* operon was amplified from *P. syringae* pv. *glycinea* B076 chromosomal DNA by using primers PsOp_Nco_F (5′-CCA TGGAGAATGACTACATCTCCGAG) and PsOp_Bgl_R (5′-TAATAAG ATCTCTCCCCAGACCCCTTCTT). The fragment was cloned into the pJet 1.2 blunt-end cloning vector (Thermo Scientific), the resulting plasmid was digested with NcoI and BglII, and *P. syringae mcb* DNA was recloned into pBAD His/B, yielding plasmid pBAD Ps-McbABCDEFG. Plasmids pBAD Ps-McbABCDEF and pBAD Ps-McbABCD were constructed in the same way, using primer pair PsOp_Nco_F and PsOp_dG_R (5′-TAGATCTTTAATTTTCTTCCAGTACCGTGG) and primer pair PsOp_Nco_F and PsOp_dEFG_R (5′-TAATAAGATCTTTACGGA AAGGGGACCATGT), respectively.

A 5.1-kb DNA fragment containing the entire *E. coli mcb* operon was amplified from plasmid pPY113 (22) by using primers EcOp_NcoF (5′-T CCATGGAATTAAAAGCGAGTGAATTTG) and EcOp_XhoR (5′-TAA TATCTCGAGTTATCCCCCTACAACCACT) and cloned into pJet 1.2. The resulting plasmid was digested with NcoI and XhoI, and the *mcb* fragment was recloned into pBAD His/B, yielding plasmid pBAD Ec-McB.

Plasmids pBAD Ps-McB I, pBAD Ps-McB II, pBAD Ps-McB III, pBAD Ec-McbA I, pBAD Ec-McbA II, and pBAD Ec-McbA III expressing chimeric *mcbA* genes were generated by using the splicing by overlapping extension (SOE) PCR method (23).

Coding regions of *P. syringae* pv. *glycinea* B076 *gyrA* and *gyrB* genes were amplified from chromosomal DNA by using primer pair PsS_GyrA_FNde (5′-TAATACATATGGGCGAACTGGCCAAA) and PsS_GyrA_RBam (5′-TAATAGGATCCTTAGTTCTGCGGTTCGTCTTCG) and primer pair PsS_GyrB_FNde (5′-TAATACATATGAGCGAAAACC AAACGTA) and PsS_GyrB_RBam (5′-TAATAGGATCCTTAGAAGTC CAGGTTGGACACTG), respectively. Amplified fragments were digested with NdeI and BamHI and cloned into pET19 to yield pET19 Ps-gyrA and pET19 Ps-gyrB.

Microcin purification and HPLC analysis. A culture (10 ml) of the producing strain was grown overnight in LB medium supplemented with 100 μg/ml ampicillin and used to inoculate 1 liter of M9 minimal medium supplemented with 0.4% sodium succinate and 100 μg/ml ampicillin. Cells were grown until the cultures reached an optical density at 600 nm (OD_{600}) of 0.6 and induced with arabinose (10 mM). The induced culture was grown for 24 h at 30°C. Cells were pelleted by centrifugation for 10 min at 4,000 × *g*, resuspended in 50 ml of 100 mM acetic acid–1 mM EDTA, and boiled for 10 min. The resulting suspension was centrifuged at 10,000 × *g*, and the supernatant was loaded onto a SepPack C_{18} cartridge (Thermo-Scientific), which was extensively washed with 10% acetonitrile–0.1% trifluoroacetic acid (TFA). Microcin-containing fractions were eluted in 8 ml of 30% acetonitrile–0.1% TFA, vacuum dried, redissolved in dimethyl sulfoxide (DMSO) and applied onto an XTerra C_{18} high-performance liquid chromatography (HPLC) column (Waters) in 10% DMSO–0.1% TFA. The column was equilibrated in 0.1% TFA. The bound material was eluted with a linear gradient of acetonitrile in 0.1% TFA (from 0 to 50% acetonitrile in 30 min). Absorbance of eluting material was monitored at 254 nm. Different forms of microcins were eluted between 12 and 16 min. Individual peaks were collected, vacuum dried, resuspended in DMSO to a final concentration of ~1 mM, and stored at −20°C. The concentration of purified microcin stocks dissolved in DMSO was measured according to methods described previously by Sinha Roy et al. (11).

MALDI-MS and MS/MS analyses. Mass spectra were recorded on an Ultraflextreme matrix-assisted laser desorption ionization–tandem time of flight (MALDI-TOF-TOF) mass spectrometer (Bruker Daltonik) equipped with an Nd laser (355 nm). The MH^+ molecular ions were measured in the reflector mode; the accuracy of the monoisotopic mass peak measurement was 0.005%. Aliquots (1 μl) of HPLC fractions were mixed on a steel target with 0.5 μl of a 2,5-dihydroxybenzoic acid (Aldrich) solution (20 mg/ml in 30% acetonitrile plus 0.5% TFA), and droplets were left to dry at room temperature. Fragment ion spectra were generated by laser-induced dissociation in lift mode; the accuracy of the mass peak measurement was 70 ppm for parent ions and 1 Da for daughter ions. The correspondence of the found masses to microcin peptides and to tandem mass spectrometry (MS/MS) peptide fragments was revealed manually with the help of GPMAW4.04 software (Lighthouse Data). A Mascot MS/MS ion search was carried out at a home server without specifying the kind of proteolysis and listing Ser-oxazole and Cys-thiazole as variable modifications.

Determination of antibiotic activity *in vivo*. Microcin stock samples were diluted to 20 to 200 μM with 50% acetonitrile, and 2-μl drops were deposited onto freshly made lawns of bacteria to be tested. Ciprofloxacin (20 μM) dissolved in water was used as a positive control. The lawns were prepared by overlaying LB agar plates with 5 ml of a 0.6% agar solution in distilled water containing 100 μl of the culture to be tested grown overnight in LB medium. Plates were incubated at room temperature overnight.

Purification of DNA gyrase. Cultures (5 ml) of *E. coli* BL21(DE3) carrying pET19 Ps-gyrA or pET19 Ps-gyrB were grown overnight in LB medium supplemented with 100 μg/ml ampicillin and were used to inoculate 0.5 liters of LB medium containing 100 μg/ml ampicillin. Cells were grown at 37°C until an OD_{600} of 0.6 was reached and were induced by adding IPTG (isopropyl-β-D-thiogalactopyranoside) to 0.2 mM. Induced cultures were grown for 16 h at 22°C. Cells were collected by centrifugation for 10 min at 4,000 × *g*, and the pellet was suspended in 15 ml of lysis buffer [20 mM Tris-HCl (pH 8), 200 mM $(NH_4)_2SO_4$, 20 mM imidazole, 10% glycerol]. Lysozyme was added to a final concentration of 1 mg/ml, and the mixture was incubated on ice for 30 min. Cells was disrupted by sonication and centrifuged at 15,000 × *g* for 30 min. The supernatant was applied onto a 0.5-ml Ni^{2+}-nitrilotriacetic acid (NTA) agarose (Qiagen) column equilibrated in lysis buffer. The column was washed extensively with wash buffer [20 mM Tris-HCl (pH 8), 200 mM $(NH_4)_2SO_4$, 50 mM imidazole, 10% glycerol], and proteins were eluted with elution buffer [50 mM Tris (pH 8.0), 200 mM $(NH_4)_2SO_4$, 10% glycerol, 300 mM imidazole].

Recombinant *E. coli* DNA gyrase subunits were purified by an analogous Ni^{2+}-NTA chromatography procedure followed by Mono Q ion-exchange chromatography, as described previously (24).

Gyrase cleavage assay. DNA cleavage assays were carried by using a method based on that described by Heddle et al. (25). Reaction mixtures contained 35 mM Tris-HCl (pH 7.5), 24 mM KCl, 4 mM $MgCl_2$, 2 mM dithiothreitol (DTT), 1.75 mM ATP, 6.5% glycerol, 1.8 mM spermidine, 0.1 mg/ml albumin, 12.5 nM relaxed pUC19 plasmid DNA, 200 nM *E. coli* or *P. syringae* DNA gyrase, and various concentrations of ciprofloxacin, *Ec*-McB, or *Ps*-McBs (in DMSO). DMSO was added to control reaction mixtures to a final concentration of 3%. Reaction mixtures were incubated for 1 h at 25°C, and reactions were terminated by the addition of SDS (to 0.2%) and proteinase K (to 0.1 mg/ml) to the mixtures, followed

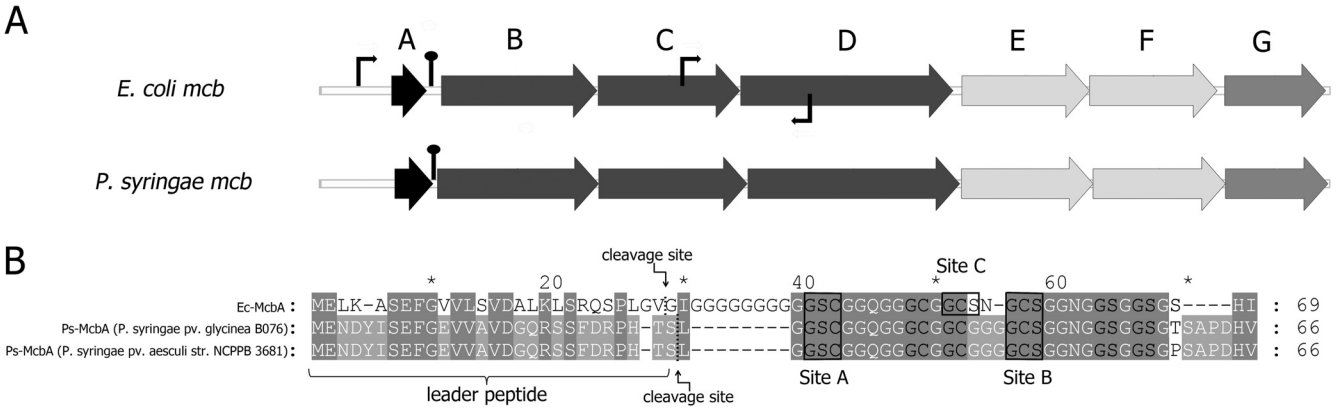

FIG 1 Cluster of *E. coli mcb* gene homologs in *P. syringae*. (A) The *E. coli mcbABCDEFG* gene cluster is schematically presented at the top, with each gene of the cluster indicated by an arrow (not drawn to scale). The *mcbBCD* genes code for microcin B synthase, the *mcbEF* genes code for the microcin B efflux pump, and *mcbG* codes for a self-immunity protein. Thin arrows indicate known *E. coli mcb* promoters (31). The homologous operon found in some strains of *P. syringae* is shown below. The extent of similarity and identity between the *E. coli* and *P. syringae* homologs ranges from 63% and 46% (for the product of *mcbC*) to 45% and 25% (for the product of *mcbG*), respectively. Hairpin-like structures between *mcbA* and *mcbB* indicate putative transcription terminators located in noncoding regions (2). (B) Alignment of *mcbA* gene products from *E. coli* (*Ec*-McbA), *P. syringae* pv. *glycinea* (GenBank accession number NZ_AEGG01000085), and *P. syringae* pv. *aesculi* (accession number ACXS01000133) (single-letter amino acid codes). The degree of background shading indicates identity in all three (dark gray) or just two (lighter gray) of the aligned polypeptides. Hyphens indicate gaps. *Ec*-McbA di- and tripeptides converted into heterocycles (and homologous residues in *P. syringae* polypeptides) are indicated by black letters. Tripeptides converted to fused cycles (site A and site B) are boxed and labeled below the alignment. An *Ec*-McbA tripeptide converted into the auxiliary site C fused cycle is boxed and labeled above the alignment. The cleavage sites between the leader and the core parts of modified *Ec*-McbA and *Ps*-McbAs are highlighted above and below the alignment, correspondingly.

by incubation at 37°C for another 30 min. Equal volumes of gel-loading buffer (40% sucrose, 100 mM Tris-HCl [pH 7.5], 1 mM EDTA, 2 mg/ml bromophenol blue) and chloroform were added to each reaction mixture. Reaction mixtures were vortexed for 1 min and centrifuged at 16,000 × *g* for 1 min. Samples were loaded onto a 1% agarose gel in TAE (40 mM Tris acetate, 1 mM EDTA) with 1 μg/ml ethidium bromide.

RESULTS

Bioinformatics identification of *E. coli mcb* gene homologs in *Pseudomonas syringae*. When we used the sequence of *E. coli* McbB (P23184), a component of the McB synthase, as a query in a BLASTP search of NCBI NR database with default parameters, several previously unreported highly similar sequences (E values of 10^{-41} or lower) were revealed. For comparison, the E value for the McbB homolog from *Pseudomonas putida* KT2440, which is the next closest homolog of *E. coli* McbB (2), is 10^{-11}. The new McbB homologs are 35% identical and 56% similar to *E. coli* McbB and are all encoded by different pathovars of *Pseudomonas syringae*. Inspection of the genomic context of *mcbB* homologs from *P. syringae* revealed the presence of an entire set of *E. coli mcb* gene homologs, *mcbA* to *mcbG* (Fig. 1A).

The putative *P. syringae* McbA peptide contains a full complement of GlySer and GlyCys dipeptides as well as the site A and site B tripeptides (Fig. 1B). However, instead of the site C tripeptide GlyCysSer present in *E. coli* McbA, the putative *P. syringae* McbA peptide contains a GlyCysGly tripeptide that can be converted to only a single thiazole cycle.

Analysis of McbA sequences encoded by different *P. syringae* pathovars reveals that they are identical to each other except for amino acid position 60, which is occupied by a threonine in strains of *P. syringae* pv. *glycinea* and a proline in strains of *P. syringae* pv. *aesculi* (Fig. 1B). Certain *P. syringae* strains, for example, *P. syringae* pv. *tomato* DC3000 or pv. *syringae* B728a, do not carry the *mcb* operon (see Table S1 in the supplemental material).

We were interested in determining whether the *mcb* operon of *P. syringae* is active, i.e., capable of producing an McB-like molecule. Patches of *P. syringae* pv. *glycinea* B076 cells were grown on LB or M9 minimal medium plates and overlaid with *P. syringae* strains lacking *mcb* or with microcin B-sensitive *E. coli* lawns. After overnight growth, no growth inhibition zones around the points of *P. syringae* pv. *glycinea* B076 growth were detected. In contrast, *E. coli* cells producing microcin B, which were used as a control, readily inhibited the growth of microcin B-sensitive *E. coli* but had no effect on the growth of *P. syringae*, which is resistant to microcin B (see also below).

We also attempted to identify secreted modified *P. syringae* McbA peptides by mass spectrometric analysis of *P. syringae* pv. *glycinea* B076 cultured medium. Since we did not know the leader peptide cleavage site, if any, in the *P. syringae* McB precursor peptide, we could not confidently predict the mass of the mature compound. Cells producing *E. coli* McB secrete not just the mature form of the peptide but also maturation derivatives containing less than the "normal" complement of 8 heterocycles (11). Since formation of a heterocycle leads to a loss of 20 Da, mass spectrometric analysis of cultured medium of McB-producing *E. coli* cells revealed a characteristic series of mass peaks differing from each other by 20-Da increments (7). Inspection of mass spectra failed to reveal such peak series within a 1- to 5-kDa mass range in cultured medium of *P. syringae* pv. *glycinea* B076. Despite the apparent absence of production of bioactive *P. syringae* pv. *glycinea* B076 *mcb* operon products, real-time PCR analysis revealed that every gene of the *mcb* operon is transcribed at a level comparable to that of an essential housekeeping gene, *gyrA* (data not shown).

Heterologous production of *P. syringae* microcin B in *E. coli*. Since we failed to detect endogenously produced *P. syringae* McB under our conditions, expression of the *P. syringae mcb* operon in *E. coli*, a heterologous host, was attempted. The entire operon was cloned into the *E. coli* expression vector under the control of the

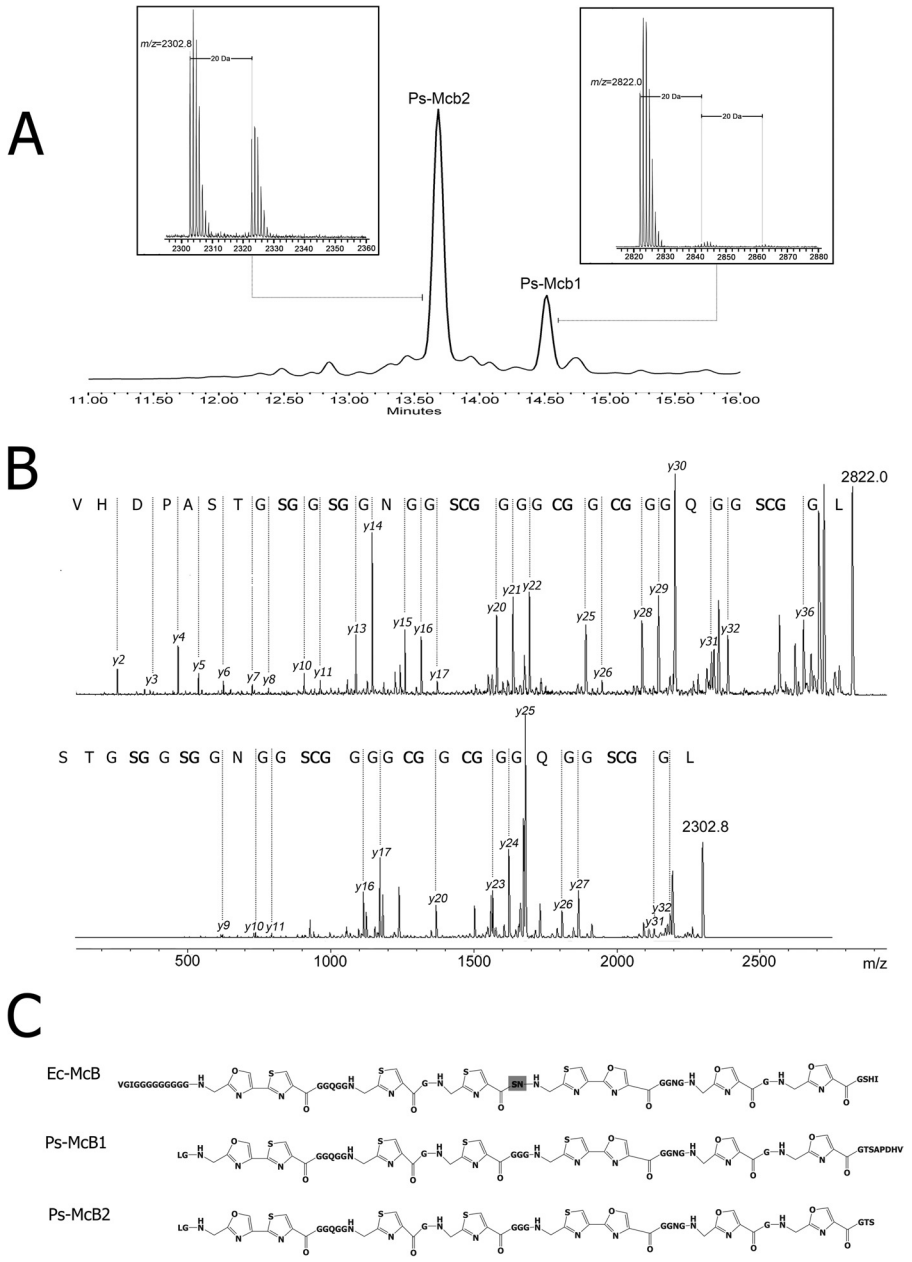

FIG 2 Characterization of *P. syringae* microcin B produced in a surrogate *E. coli* host. (A) HPLC chromatogram showing the final stage of purification from *E. coli* cells co-overexpressing the *P. syringae mcb* operon. The two peaks labeled Ps-McB1 and Ps-McB2 are absent from the control purification from cells lacking a *P. syringae mcb* operon co-overexpression plasmid. Insets show parts of MALDI-MS mass spectra of material from HPLC peaks. The *m/z* values for major mass peaks as well as +20-Da minor mass peaks are indicated. (B) MS/MS fragmentation spectra of *Ps*-McB2 (top) and *Ps*-McB1 (bottom). Both peptides fragmented well at peptide bonds and formed *b*- and *y*-ion series. The *y*-ion series was complete except for the absence of fragmentation products of peptide bonds incorporated into the heterocycles and conjugated peptide bonds lying directly downstream from some cyclized residues. These bonds were previously observed to resist fragmentation (32). (C) Structures of *Ec*-McB and of *Ps*-McB1 and *Ps*-McB1 as revealed by MS/MS analysis. The serine residue in the centrally located SN dipeptide in *Ec*-McB (highlighted with a dark gray background) undergoes an S-N shift in about 90% of *Ec*-McB molecules produced (12).

inducible *ara*P_{BAD} promoter, with the start codon of *mcbA* positioned at an optimal distance from a consensus Shine-Dalgarno sequence present in the vector. Cultured medium of arabinose-induced *E. coli* cells carrying the complete *P. syringae mcb* operon was subjected to a purification procedure developed for *E. coli* McB (11). Cultured medium from cells carrying an empty vector plasmid was used for control mock purification. During the final stage of reverse-phase HPLC, two prominent peaks were detected in material from *P. syringae mcb*-containing cells that were absent from the control (Fig. 2A). Mass spectrometric analysis revealed that the early-eluting major peak contained a primary mass ion of *m/z* 2,302.8 [MH^+] as well as a minor +20-Da mass ion of *m/z* 2,322.8 [MH^+]; the later-eluting peak contained a primary mass ion of *m/z* 2,822.0 [MH^+] and additional +20- and +40-Da mass ions (Fig. 2A). MS/MS spectra of the *m/z* 2,302.8 and 2,822.0 mass ions are presented in Fig. 2B. Analysis of the fragmentation spec-

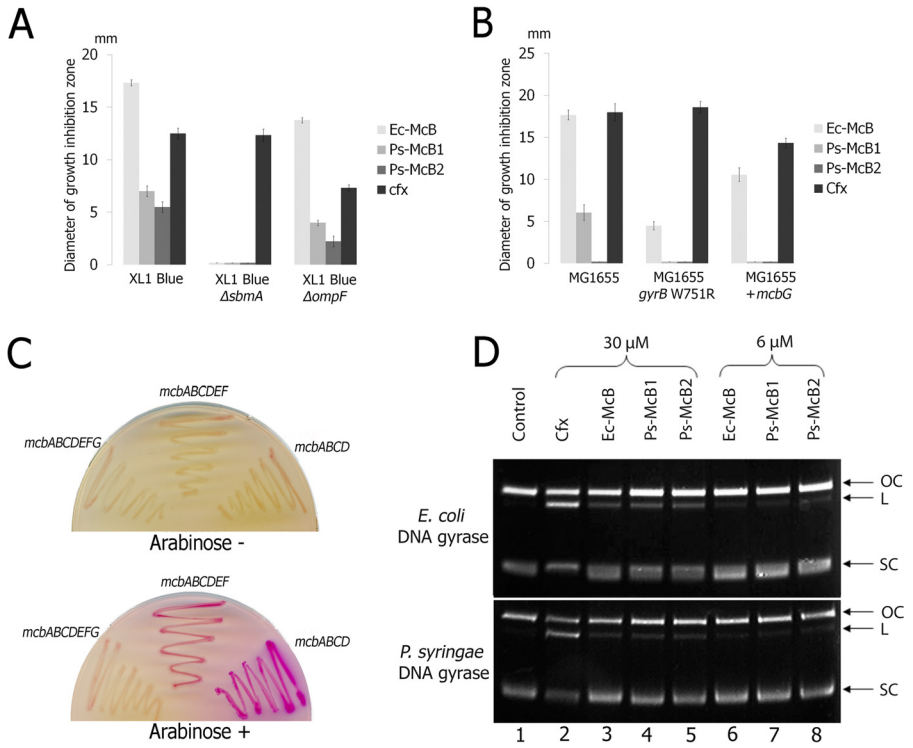

FIG 3 *In vivo* and *in vitro* activity of *Ps*-McB. (A) Two-microliter drops of solutions containing 50 μM *Ec*-McB, *Ps*-McB1, or *Ps*-McB2 or 20 μM ciprofloxacin (cfx) were deposited onto lawns of wild-type *E. coli* XL1-Blue cells or isogenic mutants lacking *sbmA* or *ompF*. After overnight growth at room temperature, diameters (in mm) of growth inhibition zones were determined. Mean values and standard deviations obtained from three independent experiments are shown. (B) Experiment performed as described for panel A, using wild-type *E. coli* MG1655 or MG1655 carrying a W751R substitution in *gyrB* (which makes cells partially resistant to *Ec*-McB) or carrying a plasmid expressing *E. coli mcbG*. (C) *E. coli* CSH50 tester cells containing an *sfiA*::*lacZ* fusion were transformed with plasmids co-overexpressing the indicated sets of *mcb* genes and plated onto MacConkey agar plates in the absence (top) or the presence (bottom) of the inducer. The results of overnight growth at 30°C are shown. (D) Plasmid pUC19 was incubated with *E. coli* or *P. syringae* gyrase in the absence or in the presence of the indicated inhibitors present at a concentration of 6 μM (lanes 6 to 8) or 30 μM (lanes 2 to 5). The reaction products were resolved by agarose gel electrophoresis and revealed by ethidium bromide staining. "OC" stands for the relaxed circular form, "L" stands for linearized plasmid, and "SC" stands for supercoiled plasmid.

trum peak series using a Mascot MS/MS ion search identification procedure was consistent with structures of cleaved and post-translationally modified *P. syringae* McbA peptides shown in Fig. 2C (identification scores of 234 and 150, respectively; scores of >76 indicate identity or extensive similarity [$P < 0.05$]). Mascot search files are presented in Tables S2 and S3 in the supplemental material.

As can be seen, both forms of modified *P. syringae* McbA have identical N termini (correspond to Leu^{29} of *P. syringae* McbA). The N termini correspond to a proteolytic event at the junction point between the predicted leader part of *P. syringae* McbA (Fig. 1) and the core part containing cyclizable di- and tripeptides. Both compounds contain eight heterocycles (four of which are present in two fused heterocycles) but differ in their C termini. Material from the minor HPLC peak has a C terminus matching that of the predicted sequence of *P. syringae* McbA. We refer to this form as *Ps*-McB1. Material from the major HPLC peak, which is referred to as *Ps*-McB2, is a C-terminally truncated variant ending at Ser^{61}. We refer to *E. coli* McB as *Ec*-McB. As noted above, the McbA peptide encoded by *P. syringae* pv. *aesculi* contains a proline instead of a threonine at position 60 (Fig. 1B). We introduced an appropriate change (P60T) into cloned *P. syringae* pv. *glycinea mcbA* and observed that *E. coli* cells expressing the altered *P. syringae mcb* operon also produced two forms of fully modified *Ps*-McB (data not shown).

***Ps*-McBs are biologically active and target the DNA gyrase.** Chromatographically pure *Ps*-McB1 and *Ps*-McB2 were prepared, and their biological activity was determined by monitoring growth inhibition zones on lawns of various tester strains (see Materials and Methods). The results are presented in Fig. 3A and B. *Ps*-McB1 was active against *E. coli* K-12 MG1655 and XL1-Blue strains, but its activity was significantly lower than the activity of equal amounts of *Ec*-McB (Fig. 3A and B). No activity of either *Ec*-McB or *Ps*-McB1 was detected on XL1-Blue cells lacking *sbmA* (Fig. 3A), an inner membrane transporter responsible for *Ec*-McB transport (26). Deletion of *ompF*, a gene coding for an outer membrane porin that participates in *Ec*-McB transport, diminished the sensitivity of XL1-Blue cells to both *Ec*-McB and *Ps*-McB1 (Fig. 3A). Thus, *Ec*-McB and *Ps*-McB1 enter *E. coli* cells through the same pathway.

No growth inhibition zones were formed by *Ps*-McB1 on lawns of MG1655 cells carrying a DNA gyrase with a Trp-to-Arg change at position 751 of the GyrB subunit ($gyrB^{Trp751Arg}$) (Fig. 3B) that renders cells partially resistant to *Ec*-McB (25). Expression of *E. coli* (Fig. 3B) or *P. syringae* (data not shown) *mcbG* from plasmids decreased the sensitivity of MG1655 cells to *Ec*-McB and made

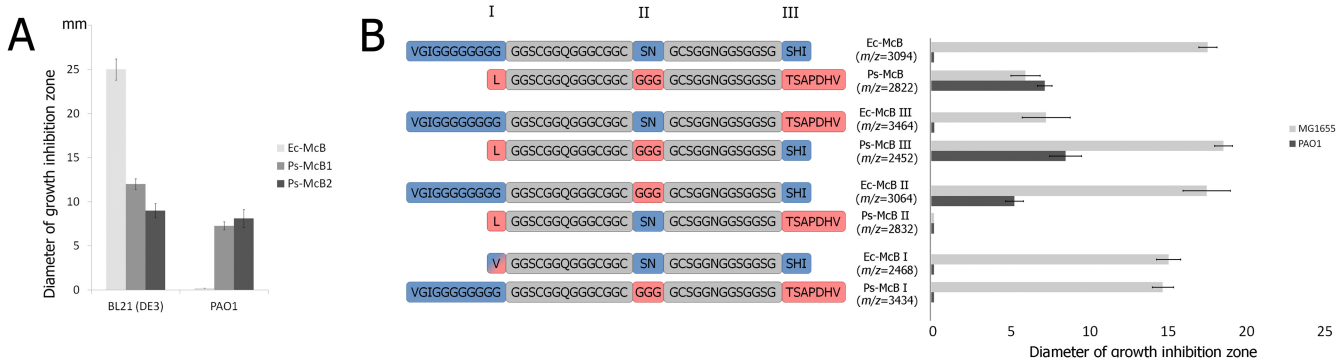

FIG 4 Species specificity of McB action. (A) Two-microliter drops of solutions containing 200 μM *Ec*-McB, *Ps*-McB1, and *Ps*-McB2 were deposited onto lawns of *E. coli* BL21(DE3) or *P. aeruginosa* PAO1. After overnight growth at room temperature, diameters of growth inhibition zones were determined. Mean values and standard deviations obtained from three independent experiments are shown. (B) Genetic constructs expressing the chimeric microcins shown on the left were prepared by swapping elements marked I, II, and III of *E. coli* and *P. syringae* microcins. Compounds containing the entire complement of heterocycles (molecular masses of compounds determined by MALDI-MS are shown in the middle and correspond to compounds with a full complement of heterocycles) were purified, and 2-μl drops of solutions containing 200 μM each compound were deposited onto lawns of *E. coli* MG1655 or *P. aeruginosa* PAO1. After overnight growth at room temperature, diameters of growth inhibition zones were determined. Mean values and standard deviations obtained from three independent experiments are shown on the right.

them resistant to *Ps*-McB1 at the concentrations used (Fig. 3B). The results thus suggest that *Ps*-McB1 targets *E. coli* DNA gyrase.

While *Ps*-McB2 was inactive against *E. coli* MG1655, a K-12 strain, at the concentrations used, it inhibited the growth of *E. coli* BL21(DE3) (Fig. 4A) and XL1-Blue (Fig. 3A), also a K-12 strain. While BL21(DE3) may be hypersensitive to *Ec*-McB and *Ps*-McBs due to increased expression of *ompF* (27), the heightened sensitivity of XL1-Blue to *Ps*-McB2 remains unexplained. Results obtained with *Ps*-McB variants carrying a proline at position 60 were identical to those reported in Fig. 3A and B (data not shown).

A plasmid carrying the *P. syringae mcb* operon under the control of the inducible *ara*P_{BAD} promoter as well as its derivatives lacking the *mcbG* gene, coding for a pentapeptide immunity protein, or both *mcbG* and *mcbEF*, which code for an export pump, were introduced into *E. coli* CSH50 *sfiA*::*lacZ* reporter cells (13) carrying a genomic fusion of the LexA-dependent *sfiA* promoter to the *lacZ* gene. When CSH50 *sfiA*::*lacZ* cells undergo the SOS response caused by accumulation of double-stranded-DNA breaks, they form red colonies on MacConkey agar indicator plates due to the relief of LexA-dependent inhibition of *sfiA*::*lacZ* fusion transcription. In the presence of arabinose, CSH50 *sfiA*::*lacZ* cells carrying a plasmid with a complete *P. syringae mcb* operon formed white colonies and cells carrying a plasmid with *mcbABCDEF* genes formed pink colonies, while cells carrying the *mcbABCD* plasmid formed purple colonies (Fig. 3C). A similar result was obtained when CSH50 *sfiA*::*lacZ* carrying *E. coli mcb* operon plasmids was tested (data not shown). The results thus indicate that the *P. syringae mcb* operon encodes a substance that promotes the SOS response in *E. coli* when the *mcbEF* and/or *mcbG* gene is disrupted.

To show directly that *Ps*-McB inhibits the DNA gyrase, its effects on plasmid DNA cleavage reactions catalyzed by DNA gyrase from *E. coli* or *P. syringae* were investigated. When DNA gyrase is incubated with relaxed plasmid DNA in the presence of ATP and inhibitors such as ciprofloxacin or *Ec*-McB, a trapped intermediate of the gyrase-catalyzed reaction, linearized plasmid DNA, is accumulated (28). Electrophoretic analysis of the products of *E. coli* or *P. syringae* DNA gyrase-catalyzed reactions conducted in the presence of 6 μM *Ec*-McB revealed the appearance of small amounts of linearized plasmid (Fig. 3D, compare lanes 6 and 1). A higher concentration of *Ec*-McB (30 μM) resulted in stronger accumulation of the linear DNA band (Fig. 3D, compare lanes 3 and 6). The linear DNA band observed in reaction mixtures containing 30 μM ciprofloxacin was much more prominent (Fig. 3D, lane 2), in agreement with previously reported data showing that fluoroquinolones are more effective inhibitors of *E. coli* DNA gyrase than *Ec*-McB (25). Importantly, the reactions conducted in the presence of either *Ps*-McB1 or *Ps*-McB2 were indistinguishable from those performed in the presence of matching concentrations of *Ec*-McB (Fig. 3D, compare lanes 7 and 8 with lane 6 and lanes 4 and 5 with lane 3). We therefore conclude that both forms of *Ps*-McB inhibit DNA gyrase *in vitro* and are approximately as potent as *Ec*-McB.

Species specificity of *Ps*-McB action. A *P. syringae* strain with the *mcb* operon (*P. syringae* pv. *glycinea* B076), two strains lacking *mcb* (*P. syringae* pv. *tomato* DC3000 and pv. *syringae* B728a), and *P. aeruginosa* PAO1 were tested for susceptibility to *Ps*-McB1, *Ps*-McB2, and *Ec*-McB (Fig. 4A) in plate lawn growth inhibition assays. *E. coli* BL21(DE3) cells were used as a control. Ciprofloxacin inhibited the growth of all bacteria tested. *Ec*-McB inhibited the growth of *E. coli* but was inactive against all *Pseudomonas* bacteria tested. In contrast, both *Ps*-McBs inhibited the growth of *P. aeruginosa* and *P. syringae* strains lacking the *mcb* operon to the same extent, while only *Ps*-McB1 demonstrated activity against *E. coli* K-12 MG1655. *P. syringae* pv. *glycinea* B076 was resistant to both forms of *Ps*-McB. We therefore conclude that *Ps*-McBs, while less potent inhibitors of the growth of *E. coli* than *Ec*-McB, are efficient inhibitors of the growth of certain pseudomonads.

Comparison of *Ec*-McB and *Ps*-McB1 revealed three areas of difference (Fig. 1B and 2C). First, *Ec*-McB contains an N-terminal $VGIG(G)_9$ sequence before the first fused heterocycle, while *Ps*-McBs contain just an LG dipeptide. Second, *Ec*-McB contains an $S^{52}N^{53}$ dipeptide between a thiazole heterocycle and the second (site B) fused heterocycle, while *Ps*-McBs contain a $G^{44}G^{45}G^{46}$ tripeptide. Finally, the C-terminal tail after the last heterocycle in *Ec*-McB is GSHI, while it is GTSAPDHV in *Ps*-McB1 (GTS in

Ps-McB2). In principle, any one of these differences or their combination can be responsible for the extended range of *Ps*-McB action. To identify the determinant(s) of the species specificity of McB action, *E. coli mcb* and *P. syringae mcb* operon-based plasmids expressing chimeric *mcbA* genes were prepared. The chimeric variants created are schematically indicated in Fig. 4B. Three *E. coli mcb*-based plasmids expressing *Ec*-McbA variants containing (i) a VG dipeptide instead of the N-terminal VGIG$(G)_9$ sequence, (ii) a GGG instead of $S^{52}N^{53}$, and (iii) C-terminal GTSAPDHV instead of GSHI were created. In addition, three *P. syringae mcb*-based plasmids expressing *Ps-mcbA* variants encoding (i) N-terminal VGIG$(G)_9$ instead of LG, (ii) SN instead of $G^{44}G^{45}G^{46}$, and (iii) C-terminal GSHI instead of GTSAPDHV were made. Compounds produced by cells carrying each of these plasmids were purified by using a standard *Ec*-McB purification procedure (11), and mass spectrometric analysis confirmed that in all cases, hybrid McBs with the full complement of heterocycles were produced (Fig. 4B). In the case of *Ec*-McB with a GTSA PDHV C-terminal tail from *Ps*-McbA, only one form, corresponding to *Ps*-McB1, was produced.

Equal amounts of chimeric compounds were placed onto lawns of *P. aeruginosa* PAO1 and *E. coli* MG1655 cells, and growth inhibition zones were recorded. A *Ps*-McB-based compound with C-terminal amino acids from *E. coli* McB was as active against *P. aeruginosa* as the parent compound and was a more potent inhibitor of *E. coli* than *Ps*-McB (in fact, this compound was at least as active as *Ec*-McB). Conversely, the *E. coli* McB-based compound with a C-terminal tail from *Ps*-McB1 remained inactive against *P. aeruginosa* and was less active against *E. coli* than *Ec*-McB. The results thus suggest that C-terminally unmodified extensions can significantly modulate the activity levels against *E. coli* but do not contribute to the species specificity of McB action.

Ec-McB with a VG dipeptide instead of the N-terminal VGIG$(G)_9$ sequence was indistinguishable from wild-type *Ec*-McB. Thus, although the N-terminal polyglycine sequence appears to be important for *Ec*-McB maturation *in vitro* (29), it is dispensable for activity, as was also recently suggested by Collin et al. (30). Furthermore, since removal of the N-terminal polyglycine sequence does not allow the *Ec*-McB-based molecule to inhibit *Pseudomonas*, it follows that it is not involved in the species specificity of McB action. Interestingly, a *Ps*-McB-based molecule containing the N-terminal VGIG$(G)_9$ sequence behaved as *Ec*-McB. The result suggests that the N-terminal extension of *Ec*-McB blocks the ability of *Ps*-McB to inhibit *Pseudomonas*, ether directly (by blocking the interaction of the hybrid molecule with machinery responsible for transport inside *Pseudomonas* cells) or indirectly (by masking a *Ps*-McB determinant of interaction with the transport machinery).

Ps-McB carrying a Ser-Asn dipeptide instead of $G^{44}G^{45}G^{46}$ lost the ability to inhibit either *E. coli* MG1655 or *P. aeruginosa* [however, this compound still inhibited the growth of the more sensitive *E. coli* BL21(DE3) cells (data not shown)]. Most importantly, *Ec*-McB with three glycines instead of $S^{52}N^{53}$ retained the ability to efficiently inhibit the growth of *E. coli* MG1655 and simultaneously acquired the ability to inhibit *P. aeruginosa*. We conclude that the presence of the central GGG tripeptide is both necessary and sufficient for inhibitory activity of McB-like compounds against *Pseudomonas*.

DISCUSSION

In this work, we characterized microcin B-like compounds encoded by some *P. syringae* strains. While the *mcb* genes are transcribed in *P. syringae*, we failed to detect production of microcin B-like compounds. On the other hand, the resistance of *P. syringae* pv. *glycinea* B076, but not of *P. syringae* lacking *mcb*, to *Ps*-McB suggests that there may be enough *mcbEFG* of *P. syringae* pv. *glycinea* B076 products expressed to account for resistance.

Production of two *Ps*-McB variants was readily observed when the plasmid-borne *P. syringae mcb* operon was introduced into a heterologous expression host, *E. coli*. The compounds produced in *E. coli* contain the full complement of heterocycles and inhibit DNA gyrase—either from *E. coli* or from *P. syringae*—*in vitro*. *Ps*-McBs enter *E. coli* through the same route as *E. coli* McB, but their antibacterial activity is lower, probably due to decreased uptake efficiency. In the case of *Ec*-McB, the N terminus of the mature compound is formed upon cleavage between the leader and the modified core part of the molecule and requires the products of the *E. coli tldD* and *tldE* genes, which probably encode proteases. The fact that the N terminus of heterologously expressed *Ps*-McB is also located at the junction site between the leader and the core part suggests that *E. coli* TldD/E may be involved in the cleavage of the modified *Ps*-McbA precursor. The *tldD* and *tldE* genes are highly conserved in eubacteria and archaea and are present in *P. syringae*. *P. syringae* TldD and TldE may be involved in *Ps*-McB maturation. However, since the specificity of these proteins is unknown, it is possible that the N termini of naturally produced *Ps*-McBs are different from those produced in surrogate hosts.

The uncertainty about their N termini notwithstanding, the heterologously produced *Ps*-McBs are biologically active and inhibit the growth of *P. syringae* strains lacking the *mcb* operon and of the human pathogen *P. aeruginosa*. *Ec*-McB is inactive against these organisms. The species specificity of McB action resides in the centrally located region of the peptide, occupied by Ser^{52} and Asn^{53} in *Ec*-McB and Gly^{44}, Gly^{45}, and Gly^{46} in *Ps*-McBs. Since both *Ec*-McB and *Ps*-McB are equally active against *E. coli* or *P. syringae* DNA gyrase *in vitro*, it follows that *Ec*-McB is unable to enter *Pseudomonas*. *Pseudomonas* genomes do not encode a recognizable homolog of SbmA (data not shown), which in *E. coli* is essential for sensitivity to *Ec*-McB. Another unrelated inner membrane transporter(s) is therefore responsible for *Ps*-McB import in *Pseudomonas*. Apparently, this transporter specifically recognizes the three consecutive glycines in the central part of *Ps*-McB but is unable to recognize Ser^{52} and Asn^{53} of *Ec*-McB, thus making *Pseudomonas* cells resistant to the latter. Since bioinformatics analysis is unable to pinpoint a *Pseudomonas* transporter responsible for *Ps*-McB sensitivity, its identification must await the results of genetic analysis. The system of *Ps*-McB production in the heterologous *E. coli* host described here allows the production of ample amounts of biologically active *Ps*-McB, which should facilitate the identification of the transport system. Bacteria of the *Pseudomonas* genus are surprisingly well endowed with operons coding for microcin B-like compounds. In addition to the *Ps*-McBs studied here, closely related operons have been detected in fully or partially sequenced genomes of *P. putida* KT2440 (2), *P. fluorescens* A506 (GenBank accession number CP003041), *P. fluorescens* NZ052 (accession number NZ_AJXH00000000), *P. fluorescens* BS2 (accession number NZ_AMZG00000000), *P. pseudoalcaligenes* KF707 (acces-

sion number AJMR01000000), and *P. tolaasii* NCPPB 2192 (accession number AJXK01000000). These operons contain a clearly recognizable cluster of *mcbABCDEF* genes but lack the distal *mcbG* gene, encoding the McB self-immunity protein. The McbA propeptides differ significantly from *E. coli* or *P. syringae* McbA polypeptides; in particular, they do not contain GlySerCys and GlyCysSer tripeptides, which are modified into oxazole-thiazole and thiazole-oxazole fused heterocycles, respectively, thought to be important for activity of *Ec*-McB (11). Characterization of compounds encoded by these operons and their targets and entry pathways as well as physiological analysis of microcin-like compound production are currently ongoing in our laboratory.

ACKNOWLEDGMENTS

We are grateful to Julia Piskunova for constructing some of the chimeric constructs used in this work. The MALDI-MS facility was made available to us within the framework of Moscow State University Development Program PNG 5.13.

This work was supported by a Molecular and Cellular Biology program grant from the Russian Academy of Sciences Presidium and a Russian Government megagrant to K.S. and Russian Foundation for Basic Research grants 13-04-01631-a to D.G. and 11-04-01846-a (to Svetlana Dubiley). M.M. is a recipient of a UMNIK contract from FASIE. D.G. is partially supported by the Dmitry Zimin Dynasty Foundation fellowship.

REFERENCES

1. **Asensio C, Perez-Diaz JC, Martinez MC, Baquero F.** 1976. A new family of low molecular weight antibiotics from enterobacteria. Biol. Biophys. Res. Commun. **69:**7–14.
2. **Severinov K, Semenova E, Kazakov A, Kazakov T, Gelfand MS.** 2007. Low-molecular-weight post-translationally modified microcins. Mol. Microbiol. **65:**1380–1394.
3. **Duquesne S, Petit V, Peduzzi J, Rebuffat S.** 2007. Structural and functional diversity of microcins, gene-encoded antibacterial peptides from enterobacteria. J. Mol. Microbiol. Biotechnol. **13:**200–209.
4. **Lee SW, Mitchell DA, Markley AL, Hensler ME, Gonzalez D, Wohlrab A, Dorrestein PC, Nizet V, Dixon JE.** 2008. Discovery of a widely distributed toxin biosynthetic gene cluster. Proc. Natl. Acad. Sci. U. S. A. **105:**5879–5884.
5. **Watrous J, Roach P, Alexandrov T, Heath BS, Yang JY, Kersten RD, van der Voort M, Pogliano K, Gross H, Raaijmakers JM, Moore BS, Laskin J, Bandeira N, Dorrestein PC.** 2012. Mass spectral molecular networking of living microbial colonies. Proc. Natl. Acad. Sci. U. S. A. **109:**1743–1752.
6. **Arnison PG, Bibb MJ, Bierbaum G, Bowers AA, Bugni TS, Bulaj G, Camarero JA, Campopiano DJ, Challis GL, Clardy J, Cotter PD, Craik DJ, Dawson M, Dittmann E, Donadio S, Dorrestein PC, Entian KD, Fischbach MA, Garavelli JS, Göransson U, Gruber CW, Haft DH, Hemscheidt TK, Hertweck C, Hill C, Horswill AR, Jaspars M, Kelly WL, Klinman JP, Kuipers OP, Link AJ, Liu W, Marahiel MA, Mitchell DA, Moll GN, Moore BS, Müller R, Nair SK, Nes IF, Norris GE, Olivera BM, Onaka H, Patchett ML, Piel J, Reaney MJ, Rebuffat S, Ross RP, Sahl HG, Schmidt EW, Selsted ME, et al.** 2013. Ribosomally synthesized and post-translationally modified peptide natural products: overview and recommendations for a universal nomenclature. Nat. Prod. Rep. **30:**108–160.
7. **Yorgey P, Lee J, Kördel J, Vivas E, Warner P, Jebaratnam D, Kolter R.** 1994. Posttranslational modifications in microcin B17 define an additional class of DNA gyrase inhibitor. Proc. Natl. Acad. Sci. U. S. A. **91:**4519–4523.
8. **Li YM, Milne JC, Madison LL, Kolter R, Walsh CT.** 1996. From peptide precursors to oxazole and thiazole-containing peptide antibiotics: microcin B17 synthase. Science **274:**1188–1193.
9. **Milne JC, Roy RS, Eliot AC, Kelleher NL, Wokhlu A, Nickels B, Walsh CT.** 1999. Cofactor requirements and reconstitution of microcin B17 synthetase: a multienzyme complex that catalyzes the formation of oxazoles and thiazoles in the antibiotic microcin B17. Biochemistry **38:**4768–4781.
10. **Garrido MC, Herrero M, Kolter R, Moreno F.** 1988. The export of the DNA replication inhibitor microcin B17 provides immunity for the host cell. EMBO J. **7:**1853–1862.
11. **Sinha Roy R, Kelleher NL, Milne JC, Walsh CT.** 1999. In vivo processing and antibiotic activity of microcin B17 analogs with varying ring content and altered bisheterocyclic sites. Chem. Biol. **6:**305–318.
12. **Ghilarov D, Serebryakova M, Shkundina I, Severinov K.** 2011. A major portion of DNA gyrase inhibitor microcin B17 undergoes an N,O-peptidyl shift during synthesis. J. Biol. Chem. **286:**26308–26318.
13. **Allali N, Afif H, Couturier M, Van Melderen L.** 2002. The highly conserved TldD and TldE proteins of Escherichia coli are involved in microcin B17 processing and in CcdA degradation. J. Bacteriol. **184:**3224–3231.
14. **Mitchell DA, Lee SW, Pence MA, Markley AL, Limm JD, Nizet V, Dixon JE.** 2009. Structural and functional dissection of the heterocyclic peptide cytotoxin streptolysin S. J. Biol. Chem. **284:**13004–13012.
15. **Qi M, Wang D, Bradley CA, Zhao Y.** 2011. Genome sequence analyses of Pseudomonas savastanoi pv. glycinea and subtractive hybridization-based comparative genomics with nine pseudomonads. PLoS One **6:**e16451. doi: 10.1371/journal.pone.0016451.
16. **Miller JH.** 1972. Experiments in molecular genetics. Cold Spring Harbor Laboratory, Cold Spring Harbor, NY.
17. **Datsenko KA, Wanner BL.** 2000. One-step inactivation of chromosomal genes in Escherichia coli K-12 using PCR products. Proc. Natl. Acad. Sci. U. S. A. **97:**6640–6645.
18. **Stover CK, Pham XQ, Erwin AL, Mizoguchi SD, Warrener P, Hickey MJ, Brinkman FS, Hufnagle WO, Kowalik DJ, Lagrou M, Garber RL, Goltry L, Tolentino E, Westbrock-Wadman S, Yuan Y, Brody LL, Coulter SN, Folger KR, Kas A, Larbig K, Lim R, Smith K, Spencer D, Wong GK, Wu Z, Paulsen IT, Reizer J, Saier MH, Hancock RE, Lory S, Olson MV.** 2000. Complete genome sequence of Pseudomonas aeruginosa PAO1, an opportunistic pathogen. Nature **406:**959–964.
19. **Joardar V, Lindeberg M, Jackson RW, Selengut J, Dodson R, Brinkac LM, Daugherty SC, Deboy R, Durkin AS, Giglio MG, Madupu R, Nelson WC, Rosovitz MJ, Sullivan S, Crabtree J, Creasy T, Davidsen T, Haft DH, Zafar N, Zhou L, Halpin R, Holley T, Khouri H, Feldblyum T, White O, Fraser CM, Chatterjee AK, Cartinhour S, Schneider DJ, Mansfield J, Collmer A, Buell CR.** 2005. Whole-genome sequence analysis of Pseudomonas syringae pv. phaseolicola 1448A reveals divergence among pathovars in genes involved in virulence and transposition. J. Bacteriol. **187:**6488–6498.
20. **Feil H, Feil WS, Chain P, Larimer F, DiBartolo G, Copeland A, Lykidis A, Trong S, Nolan M, Goltsman E, Thiel J, Malfatti S, Loper JE, Lapidus A, Detter JC, Land M, Richardson PM, Kyrpides NC, Ivanova N, Lindow SE.** 2005. Comparison of the complete genome sequences of Pseudomonas syringae pv. syringae B728a and pv. tomato DC3000. Proc. Natl. Acad. Sci. U. S. A. **102:**11064–11069.
21. **Buell CR, Joardar V, Lindeberg M, Selengut J, Paulsen IT, Gwinn ML, Dodson RJ, Deboy RT, Durkin AS, Kolonay JF, Madupu R, Daugherty S, Brinkac L, Beanan MJ, Haft DH, Nelson WC, Davidsen T, Zafar N, Zhou L, Liu J, Yuan Q, Khouri H, Fedorova N, Tran B, Russell D, Berry K, Utterback T, Van Aken SE, Feldblyum TV, D'Ascenzo M, Deng WL, Ramos AR, Alfano JR, Cartinhour S, Chatterjee AK, Delaney TP, Lazarowitz SG, Martin GB, Schneider DJ, Tang X, Bender CL, White O, Fraser CM, Collmer A.** 2003. The complete genome sequence of the Arabidopsis and tomato pathogen Pseudomonas syringae pv. tomato DC3000. Proc. Natl. Acad. Sci. U. S. A. **100:**10181–10186.
22. **Genilloud O, Moreno F, Kolter R.** 1989. DNA sequence, products, and transcriptional pattern of the genes involved in production of the DNA replication inhibitor microcin B17. J. Bacteriol. **171:**1126–1135.
23. **Horton RM, Hunt HD, Ho SN, Pullen JK, Pease LR.** 1989. Engineering hybrid genes without the use of restriction enzymes: gene splicing by overlap extension. Gene **77:**61–68.
24. **Reece RJ, Maxwell A.** 1991. Probing the limits of the DNA breakage-reunion domain of the Escherichia coli DNA gyrase A protein. J. Biol. Chem. **266:**3540–3546.
25. **Heddle JG, Blance SJ, Zamble DB, Hollfelder F, Miller DA, Wentzell LM, Walsh CT, Maxwell A.** 2001. The antibiotic microcin B17 is a DNA gyrase poison: characterisation of the mode of inhibition. J. Mol. Biol. **307:**1223–1234.
26. **Laviña M, Pugsley AP, Moreno F.** 1986. Identification, mapping, cloning and characterization of a gene (sbmA) required for microcin B17 action on Escherichia coli K12. J. Gen. Microbiol. **132:**1685–1693.
27. **Han MJ, Lee SY, Hong SH.** 2012. Comparative analysis of envelope proteomes in Escherichia coli B and K-12 strains. J. Microbiol. Biotechnol. **22:**470–478.
28. **Vizán JL, Hernández-Chico C, del Castillo I, Moreno F.** 1991. The

peptide antibiotic microcin B17 induces double-strand cleavage of DNA mediated by E. coli DNA gyrase. EMBO J. **10:**467–476.
29. **Sinha Roy R, Belshaw PJ, Walsh CT.** 1998. Mutational analysis of posttranslational heterocycle biosynthesis in the gyrase inhibitor microcin B17: distance dependence from propeptide and tolerance for substitution in a GSCG cyclizable sequence. Biochemistry **37:**4125–4136.
30. **Collin F, Thompson RE, Jolliffe KA, Payne RJ, Maxwell A.** 2013. Fragments of the bacterial toxin microcin b17 as gyrase poisons. PLoS One **8:**e61459. doi:10.1371/journal.pone.0061459.
31. **Moreno F, Gónzalez-Pastor JE, Baquero MR, Bravo D.** 2002. The regulation of microcin B, C and J. operons. Biochimie **84:**521–529.
32. **Belshaw PJ, Roy RS, Kelleher NL, Walsh CT.** 1998. Kinetics and regioselectivity of peptide-to-heterocycle conversions by microcin B17 synthetase. Chem. Biol. **5:**373–384.